

My Health Sensor, my Classifier – Adapting a Trained Classifier to Unlabeled End-User Data

Konstantinos Nikolaidis ^{*1}, Stein Kristiansen¹, Thomas Plagemann¹, Vera Goebel¹,
Knut Liestøl¹, Mohan Kankanhalli², Gunn Marit Traaen^{3,4,5}, Britt Øverland⁶,
Harriet Akre^{4,10}, Lars Aakerøy^{7,8}, and Sigurd Steinshamn^{7,8}

¹Department of Informatics, University of Oslo, Norway

²Department of Computer Science, National University of Singapore, Singapore

³Department of Cardiology, Oslo University Hospital, Rikshospitalet, Oslo, Norway

⁴Institute of Clinical Medicine, Faculty of Medicine, University of Oslo, Oslo, Norway

⁵KG Jebsen Center for Cardiac Research, University of Oslo, Norway and Center for Heart Failure Research, Oslo University Hospital, Norway

⁶Department of Otorhinolaryngology, Head & Neck Surgery, Sleep Unit, Lovisenberg Diakonale Hospital, Oslo, Norway

⁷Department of Thoracic Medicine, St. Olavs University Hospital, Trondheim, Norway

⁸KG Jebsen Center of Exercise in Medicine, Department of Circulation and Medical Imaging, Faculty of Medicine and Health Science, Norwegian University of Science and Technology, Trondheim, Norway.

⁹Department of Cardiology and Center for Cardiological Innovation, Oslo University Hospital, Rikshospitalet, Oslo, Norway

¹⁰Department of Otorhinolaryngology, Head & Neck Surgery, Oslo University Hospital, Rikshospitalet, Oslo, Norway

October 12, 2021

Abstract

In this work, we present an approach for unsupervised domain adaptation (DA) with the constraint, that the labeled source data are not directly available, and instead only access to a classifier trained on the source data is provided. Our solution, iteratively labels only high confidence sub-regions of the target data distribution, based on the belief of the classifier. Then it iteratively learns new classifiers from the expanding high-confidence dataset. The goal is to apply the proposed approach on DA for the task of sleep apnea detection and achieve personalization based on the needs of the patient. In a series of experiments with both open and closed sleep monitoring datasets, the proposed approach is applied to data from different sensors, for DA between the different datasets. The proposed approach outperforms in all experiments the classifier trained in the source domain, with an improvement of the kappa coefficient that varies from 0.012 to 0.242. Additionally, our solution is applied to digit classification DA between three well established digit datasets, to investigate the generalizability of the approach, and to allow for comparison with related work. Even without direct access to the source data, it achieves

*Corresponding Author: konstan@ifi.uio.no

good results, and outperforms several well established unsupervised DA methods.

1 Introduction

In the context of Machine Learning, Domain Adaptation (DA) has recently been successfully applied to address the problem of shift across different domains. DA aims to improve learning for a predictive task at a target, assuming a source and a target domain for which the distributions of source and target differ [1, 2]. The predictive tasks are the same across the two domains. A sub-field of DA is unsupervised DA, for which labels are provided only for the source data [3], but not for the target data.

However, there are use-cases in which the source data cannot be used together with the target data. Consider in a medical setting a scenario in which a patient collects health data with a smartwatch. Health data is typically examined by a medical expert to detect a certain health condition or its absence. Recent research results have shown that Machine Learning can successfully be used for such tasks like sleep apnea detection [4, 5, 6]. However, training to create such a classifier can be difficult because, in a supervised setting, experts are required to label the data and the classifier needs to be personalized for each individual. The latter is necessary because individuals are different in terms of physiology, prevalence, sensor placement and the same signals might be measured with different sensors, for example different smartwatch brands.

In our lab, we face a similar scenario. We aim to develop machine learning solutions for sleep monitoring to identify signs of sleep apnea. Sleep apnea is a severe disorder that is rather common, but unfortunately strongly under-diagnosed. To enable “anybody” to use such solutions at home, the data shall be collected with low-cost consumer electronics, including smart phones and smart watches. We use as foundation for our research data from a large clinical study, called A3 study, at the Oslo University Hospital and St. Olavs University Hospital. In this study, sleep monitoring data from several hundred patients is collected and analyzed. A portable sleep monitor certified for clinical diagnosis (i.e., Nox T3) has been used for data acquisition. Currently, we achieve with a CNN trained on this data a classification accuracy of approximately 80%. However, we cannot guarantee that this model can generalize well to new data from an end-user, because of potential domain shifts. Such domain shifts can for example be caused by characteristics of individual end-user sleep data that are not represented in the A3 dataset and quality issues. The latter is based on the fact that a sleep monitor that is certified for clinical diagnosis produces data with substantially higher quality than that of data collected by end-users at home with consumer electronics. Existing Domain Adaptation solutions cannot be applied to create a classifier that is adapted to the end-user data, because (1) end-users might not want to give us their data for privacy reasons and we do not have the resources to support many end-users, and (2) privacy regulations do not permit to share the A3 dataset (e.g., with end-users or third parties).

This scenario can be generalized. Assume a host which has trained a model with labeled data for classification, but the model cannot be directly used on data collected by an end-user due to the presence of domain shift. Both entities, i.e., host and end-user do not want (or cannot) share their data with the other entity. Thus, the only way to create a personalized classifier for the end-user is DA without direct access to the labeled source data. Furthermore, it must be considered that the end-user potentially has less computing resources than the host (e.g., lack of dedicated hardware components, lack of sufficient GPU memory to load the data, etc). As a result even if the host is willing to share her data, performing joint training on the end-user could be problematic.

To address these issues, we introduce *Step-wise Increasing target Dataset Coverage based on high confidence (SICO)* to efficiently perform DA at the end-user. *SICO* performs unsupervised DA with the use of only a classifier trained on the source domain and unlabeled data from the target domain. One of the fundamental ideas in this work is to release only the classifier trained on the source domain, since extracting personal information from a classifier, especially for time series data, is harder than having direct access to the true data of the individual.¹ At the same time, since the training will be done at the end-user, we take into account possible lack of hardware resource capabilities. By using only a single trained classifier and only the data from the end-user, the proposed approach is less resource intensive than normal unsupervised DA.

Based on this, the contributions of this work include: (1) the introduction of *SICO*, a DA technique which leverages the neuronal excitation of the output neurons as a means to iteratively select high confidence regions to train with. The goal of this process is to incrementally address the existing domain shift, and generalize well to the data of the end-user. (2) The application of the proposed approach on the real-world problem that we are interested in, namely sleep apnea detection and the investigation of the effectiveness for different physiological sensors and datasets. (3) The investigation of the proposed approach to perform DA for a different type of data and for a different task (i.e., digit classification), which showcases its generalizability.

2 Method

In this section, we describe the proposed approach, and provide some insights about how and why it works.

2.1 Step-Wise Increasing Target Dataset Coverage based on High Confidence

In this work, we assume that h_{src} is trained with data from a host with a labeled dataset D_{src} (see Figure 1), and afterwards is released to the public. An end-user has an unlabeled dataset D_{tg} and wants to classify D_{tg} on the same *task*

¹However it is not impossible to extract private information from a model [7]. As on-going work we investigate to introduce privacy guarantees in the form of differential privacy.

[1] that h_{src} has been trained for. The goal of *SICO* is, given h_{src} , to create a new classifier h_{tg} that is adapted to D_{tg} .

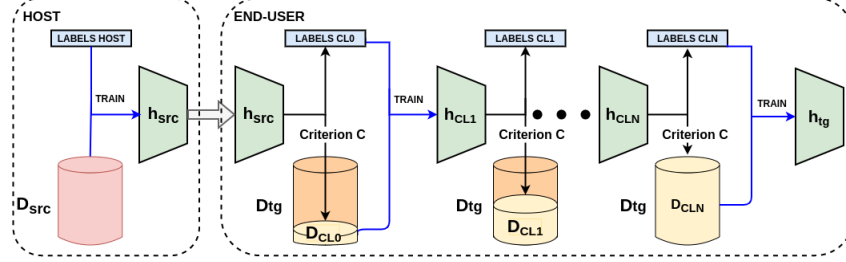


Figure 1: In the proposed method, we train h_{src} on D_{src} , and we release it to the end-user (target). The end-user incrementally adapts new classifiers to their domain based on the iterative beliefs of $h_{src}, h_{CL1} \dots h_{CLN}$ and a criterion C .

We assume that h_{src} is a neural network which performs density estimation of the true conditional distribution $p(y|x)$. The core idea of the proposed approach (see Figure1) is to start with the data of the host D_{src} , and then train and release h_{src} with D_{src} . Then, assuming that the end-user has access to an unlabeled dataset D_{tg} , we select the subset of D_{tg} that satisfies a criterion $C\{h_{src}\}$, which we will call D_{CL0} . This subset consists of the data for which, depending on the formulation of C , h_{src} is highly confident about their true label. Thus, we use h_{src} to label D_{CL0} , and train a new classifier h_{CL1} on D_{CL0} with these labels. We repeat the procedure with h_{CL1} labelling from the remaining data of $D_{tg} - D_{CL0}$ in order to create a new dataset D_{CL1} consisting of D_{CL0} together with all the data that satisfy $C\{h_{CL1}\}$ from $D_{tg} - D_{CL0}$. We then train h_{CL2} from D_{CL1} . We repeat these steps until a terminal condition is being met. In algorithmic form, the method includes the following steps:

- **Step 1:** We train h_{src} on D_{src} and release h_{src} to the public
- **Step 2:** Based on a given confidence criterion $C\{h_{src}\}$ (for example that the logits of the classifier for a class are larger than a threshold T) choose a subset $D_{CL0} \subset D_{tg}$ such that $C\{h_{src}\}$ is satisfied $\forall \mathbf{x}_T^i \in D_{CL0}$.
- **Step 3:** Based on the labels Y_{CL0} that h_{src} produces for D_{CL0} train a new classifier h_{CL1} with D_{CL0} and Y_{CL0}
- **Step 4:** Set $i = 1$. Repeat **Steps 5, 6** and **7** until $D_{CLi} = D_{tg}$, or until a terminal condition is met (e.g., $i \leq N$).
 - **Step 5:** Based on $C\{h_{CLi}\}$ choose D_{CLi} such that $D_{CL(i-1)} \subset D_{CLi} \subseteq D_{tg}$. D_{CLi} is defined as the subset: $D_{CLi} = ((D_{tg} - D_{CL(i-1)}) \text{ s.t } C\{h_{CLi}\}) \cup D_{CL(i-1)}$. Thus, D_{CLi} contains all $D_{CL(i-1)}$ together with all the datapoints of $(D_{tg} - D_{CL(i-1)})$ which satisfy $C\{h_{CLi}\}$.
 - **Step 6:** Use h_{CLi} to label $(D_{CLi} - D_{CL(i-1)})$. Unite with $Y_{CL(i-1)}$ to create Y_{CLi}

- **Step 7:** Based on the labels Y_{CLi} that $h_{CLj}, j = src, 1, \dots, i$ have produced for D_{CLi} train a new classifier $h_{CL(i+1)}$ with D_{CLi} and Y_{CLi} . Set $i = i + 1$.

- **Step 8:** Return $h_{tg} = h_{CLi}$

Please note that choosing a good criterion C is vital for the success of the algorithm. If we choose improper C and we have a demanding terminal condition to meet (like having a high threshold of belief $\forall \mathbf{x}_T^i \in D_{tg}$), the algorithm could "get stuck", or the performance could suffer. In the next subsections we discuss potential choices for C .

2.2 Methodological Analysis

We need two core characteristics for the method to work well: (1) We need h_{src} to be sufficiently trustworthy such that if we satisfy $C\{h_{src}\}$ for a given \mathbf{x}_T^i (a datapoint from the input space), there is a high probability that \mathbf{x}_T^i belongs to the true class that h_{src} predicts. Thus, if the data distributions of the host and the end-user are very different, it is clear that we cannot expect very good performance either from h_{tg} , or from h_{src} . This observation is in-line with the theoretical analysis for domain adaptation from [8] (see Theorem 1). (2) We need h_{CLi} to be trained on a subset of D_{tg} with labels for which we are confident to generalize to new data from D_{tg} with high confidence. This is equivalent to a classifier generalizing well to new data. Thus, the design of h_{CLi} needs to be good enough, and also the dataset $D_{CL(i-1)}$ with which h_{CLi} has been trained should be large enough to give h_{CLi} the ability to generalize well. This characteristic, i.e., (2) is needed for all the classifiers during the algorithm.

At the last step of the algorithm, the empirical risk of h_{tg} (for cross-entropy loss) for the last dataset $D_{CLn} \subseteq D_{tg}$ is:

$$\hat{L}(h_{tg}) = -\frac{1}{|D_{CLn}|} \sum_{\mathbf{x}_T^j \in D_{CLn}} \sum_c y_{j,CLi}^c \log(h_{tg}^c(\mathbf{x}_T^j))$$

where $y_{j,CLi}^c$ is the element c of the one-hot encoded-vector of $\argmax_c \{h_{CLi}^c(\mathbf{x}_T^j)\}$, with $i \in \{0, n\}$, the index for the classifier which labelled \mathbf{x}_T^j , and 0 referring to h_{src} . Notice that it is not necessary that $D_{CLn} = D_{tg}$ as we could stop the algorithm before the criterion holds for the whole D_{tg} . We have for the true empirical risk of h_{tg} , with the true labels:

$$\begin{aligned} L(h_{tg}) &= -\frac{1}{|D_{CLn}|} \sum_{\mathbf{x}_T^j \in D_{CLn}} \sum_c y_j^c \log(h_{tg}^c(\mathbf{x}_T^j)) \\ &= -\frac{1}{|D_{CLn}|} \sum_{\mathbf{x}_T^j \in D_{CLn}} \sum_c y_{j,CLi}^c \log(h_{tg}^c(\mathbf{x}_T^j)) - \frac{1}{|D_{CLn}|} \sum_j \delta_j \cdot \log(h_{tg}(\mathbf{x}_T^j)) \\ &= \hat{L}(h_{tg}) + \frac{1}{|D_{CLn}|} \Delta(h_{tg}) \end{aligned} \tag{1}$$

with $\delta_j = y_j - y_{j,CLi}$, and y_j the true label vector of \mathbf{x}_T^j . Notice that when $y_j = y_{j,CLi}$, $\delta_j = \mathbf{0}$. Intuitively, Δ can be thought as a form of accumulative error of the algorithm, and the larger it is the bigger the difference of the true loss and the actual loss we are minimizing. This obviously has a negative impact in the performance on new data.

Additionally, notice that from the above algorithm, in the labels Y_{CLi} for a dataset D_{CLi} there are as many errors expected as there are made from h_{CLi} 's generalization, plus the errors that were "passed" from the generalizations of the previous classifiers. However, h_{CLi} 's generalization error is also dependent on the generalization error from the previous classifiers, because it uses $D_{CL(i-1)}$ for training with the labels of the previous classifiers. Based on this discussion, and assuming that we use n classifiers, Δ can be rewritten recursively in the following form:

$$\begin{aligned}
\Delta(h_{tg}) &= \Delta_n(h_{tg}; h_{src}, h_{CL1} \dots h_{CLn}) \\
&= - \sum_{\mathbf{x}_T^j: y_j \neq y_{j,CLi}} \delta_j \cdot \log(h_{tg}(\mathbf{x}_T^j)) \\
&= - \sum_{\mathbf{x}_T^j \in (D_{CLn} - D_{CL(n-1)})} \delta_j(h_{src}, h_{CL1} \dots h_{CLn}) \cdot \log(h_{tg}(\mathbf{x}_T^j)) \\
&\quad + \Delta_{n-1}(h_{tg}; h_{src}, h_{CL1} \dots h_{CL(n-1)})
\end{aligned} \tag{2}$$

where we define as $\Delta_0(h_{tg}; h_{src}) = - \sum_{\mathbf{x}_T^j \in D_{CL0}} \delta_j(h_{src}) \cdot \log(h_{tg}(\mathbf{x}_T^j))$. From this form it is straightforward that the earlier classifiers play a more important role in the performance of h_{tg} , since their error in a sense "propagates" through the next training iterations. Thus, h_{src} plays the most important role as the first classifier in the algorithm.

Furthermore, for every step i of the algorithm, the generalization capability of the classifier h_{CLi} plays an important role in the accumulative Δ . If h_{CLi} 's generalization capability is low, it will assign many erroneous labels during the labeling of its high confidence dataset for criterion $C\{h_{CLi}\}$. This will also affect the next steps, since we have to expect worse generalization capability for the next classifiers, because these data will become training data to the next classifier etc. Finally, notice that the above analysis can be applied to any h_{CLi} and its respective $D_{CL(i-1)}$ instead of h_{tg} and D_{CLn} .

2.3 Choosing the Belief Criterion

An essential part of the proposed method is the criterion C with which we choose for a classifier h_{CLi} the new subset of D_{tg} to include to $D_{CL(i-1)}$, i.e., $(D_{CLi} - D_{CL(i-1)})$. We label this part with h_{CLi} , and then combine it with $D_{CL(i-1)}$ and use to train $h_{CL(i+1)}$. In our case, we assume that all h_{CLi}, h_{src}, h_{tg} are neural networks with softmax output. We therefore take advantage of the neuronal excitation of the output class neurons. We use neuronal excitation as an indication of confidence that \mathbf{x}_T^i belongs to a class.

There are many ways we can use the excitation of the output neurons as a criterion to assign labels for a high confidence sub-dataset. Examples include thresholding, selecting the m datapoints which lead to the strongest activation for each class neuron, or if the class of an output neuron becomes the maximum class for m datapoints, pick the $m/100$ datapoints that activate this neuron the most, etc.

2.4 *SICO* and Curriculum Learning

At first glance *SICO* and Curriculum Learning (CL) [9] can appear to be quite similar. In CL the training "starts small" by using a small training set with easy examples identified with the use of a scoring function [10]. Afterwards, CL progressively utilizes more difficult examples which are added to the curriculum. Similarly, we utilize easier examples in terms of domain similarity, and progressively train with harder datapoints. The previous classifier's class probabilities give us a measurement of the datapoints that are easier for the classifier in terms of the classifiers' higher confidence regarding these points (lower entropy). We hypothesize that datapoints that are easier -in terms of lower entropy- for a classifier trained in a different domain are more likely to be more similar to datapoints from the source domain, in terms of class separation.

However, the basic vanilla CL uses a static scoring function during training. *SICO* utilizes instead a sequence of scoring functions (i.e., h_{CLi}) that are learned dynamically as the training process continues. The creation of a new scoring function depends on the dataset and the previous scoring function. Additionally, the first scoring function, i.e., h_{src} , is independently trained and acts as a Teacher that provides the initial scoring paradigm, in conjunction with the belief criterion used. We compare our method with other more relevant and recent works of CL for DA in Section 6.

3 Experiment Description

The main goal of this work is to perform successful domain adaptation for bio-sensory signals for the purpose of sleep apnea detection. Additionally, we complement the physiological datasets with datasets for digit classification, i.e., USPS, MNIST, SVHN for two reasons. First, the majority of the related literature uses these datasets and so they serve as a baseline for comparison. Second, we want to investigate the generalizability of our approach for different types of data.

In the next subsections, we describe the datasets used and discuss the experimental set-up.

3.1 Datasets

We use the following six datasets to evaluate *SICO*:

- **MNIST** [11] (M) is a dataset containing 60000 28×28 images of digits (handwritten black and white images of 0-9) as a training set. The test set comprises of 10000 images.
- **USPS** [12] (U) is another handwritten digit dataset (0-9), which contains 7291 grayscale 16×16 training and 2007 test images.
- **SVHN** [13]: (S) is a real-world image dataset obtained from house numbers in Google Street View images. Similarly to the previous datasets, classification is performed for digits 0-9. It contains 73257 digits (32×32 colored images) for training, 26032 digits for testing, and 531131 additional training data. We use only the original training dataset of 73257 digits.
- **Apnea-ECG** [14] (AE) is an open dataset from Physionet, containing sensor data from chest respiration, abdomen respiration, nasal airflow (NAF), oxygen saturation and Electrocardiograph (ECG). AE has been used in the Computers in Cardiology challenge [14] and it contains high quality data. It has been collected with Polysomnography in a sleep laboratory. From the 35 ECG recordings in the dataset, 8 recordings (from 8 different patients) contain data from all the sensors. Each recording has duration of 7-10 hours. The sampling frequency of all sensors is 100Hz, and labels are given for every one-minute window of breathing. The labels identify which minutes are apneic and which are not (i.e., if a person experiences an apneic event during this minute). From AE , we use the NAF, chest respiration, and oxygen saturation signals.
- **MIT-BIH** [15] (MB) is an open dataset containing recordings from 18 patients. The recordings contain different respiratory sensor signals. In 15 recordings, the respiratory signal has been collected with NAF. For this reason, we focus on the NAF signal for the MB dataset. Due to misalignment of the different signals and lack of labels for the apneic class in 4 recordings, we utilize 11 of the 15 recordings (slp60, slp41 and slp45 and slp67x are excluded). It is important to note that the data/labelling quality of the MB dataset is low, which leads to low classification performance for MB compared to the other respiratory datasets that we investigate [4]. The labels are given for every 30 seconds and the sampling frequency of all sensors is 250Hz.
- The **A3 study** [16] ($A3$) investigates the prevalence, characteristics, risk factors and type of sleep apnea in patients with paroxysmal atrial fibrillation. The data were obtained with the use of the Nox T3 sleep monitor with mobile sleep monitoring at home, which in turn results into lower data quality than data from polysomnography in sleep-laboratories. An experienced sleep specialist scored the recordings manually using Noxturnal software such that the beginning and end of all types of apnea events is marked in the time-series data. To use the data for the experiments in this paper, we labeled every 60 second window of the data as apneic (if an apneic event happened during this time window) or as non-apneic.

The data we use in the experiments is from 438 patients and comprises 241350 minutes of sleep monitoring data. The ratio of apneic to non-apneic windows is 0.238. We use only the NAF signal from the A3 data in the experiments, i.e., the same signal we use from Apnea-ECG.

3.2 Preprocessing

The data in all sleep apnea datasets is standardized (per physiological signal), downsampled to 1Hz and the windows are shuffled randomly. The data from the A3 study, are very unbalanced, i.e., it contains many more non-apneic than apneic one-minute windows. Therefore, we rebalance the dataset to contain equal amount of apneic and non-apneic one-minute windows. Since the labels in *MB* are given every 30 seconds, while *AE* and *A3* are labeled every 60 seconds, we adapt the labelling in *MB* to 60 seconds by using the following rule: if both 30 second labels are non-apneic then the 60 seconds label is non-apneic, otherwise it is apneic. For *A3*, we use 80% of data as training and 20% as test set. For *AE* we use 25% of the data as test set, and for *MB* we use 15% of the data as test set. We use less test set data for *MB* because we want to utilize more data for training due to the low quality.

We rescale the data in all digit classification datasets from 0-255 to 0-1. Additionally, for *U* and *S*, we restructure the data so that it is in similar form to the *M* data. We up-scale the images in *U* from 16×16 to 28×28 , and we downscale the images in *S* from 32×32 to 28×28 . Additionally, we convert the color images in *S* to grayscale images.

3.3 Experimental Set-Up

We follow in the experiments the steps outlined in Section 2, i.e., we train h_{src} such that it can generalize well for the test set of D_{src} and release h_{src} to the end-user. Then we use h_{src} and a subset of D_{tg} to iteratively create h_{tg} . The performance of h_{tg} is evaluated with the test set of D_{tg} . This means that we evaluate the proposed method on the test set of D_{tg} . We use the convention $D_{src} \rightarrow D_{tg}$ to indicate that h_{src} is trained on D_{src} and h_{tg} is evaluated on D_{tg} . For each experiment we describe the core algorithmic decisions (e.g. the belief criteria). Further details about other minor algorithmic decisions can be found in Appendix A. Since D_{tg} is not labeled, we do not have access to a validation set during the training of the proposed method. Thus, we train each classifier h_{CLi} for a fixed number of batch iterations.

3.3.1 Belief Criteria

We empirically investigated to use a fixed threshold for the choice of high confidence data. However, this did not perform well, since the trained classifiers which are transferred from the source domain have biases towards certain classes in the target domain. This results in unbalanced D_{CLi} , which negatively affects the performance. For this reason, we select the m datapoints per-class which

excite the class output neurons the most as belief criterion $C\{h\}$ in all experiments (except $M \rightarrow U$). We use this criterion in order to maintain the class balance since all datasets with the exception of U that are used as D_{tg} are relatively well-balanced. Since U is not well balanced, we choose a criterion that gives more "freedom" to the classifier to perform the balancing. Instead of choosing an absolute number N , as $C\{h\}$, we select a percentage p of the datapoints which activate a class output neuron the most.

4 Experiments and Results

The first set of experiments evaluates *SICO* for digit classification and investigates three combinations that are commonly used in literature, i.e., $M \rightarrow U$, $U \rightarrow M$, $S \rightarrow M$. The second set of experiments focuses on sleep apnea detection with physiological sensors. The application scenario that we are interested in focuses on the transition from high quality sensor data to low quality sensor data. Additionally, we investigate combinations for which the low quality data are used as D_{src} , in order to get a more complete picture of the capabilities of the proposed algorithm. We focus on the NAF signal for the combinations $A3 \rightarrow AE$, $A3 \rightarrow MB$, $MB \rightarrow AE$, $AE \rightarrow MB$, $AE \rightarrow A3$, and evaluate the abdominal respiration, the chest respiration and the oxygen saturation sensor signals for the $A3 \rightarrow AE$ and $AE \rightarrow A3$ combinations.

Figures 2 and 3 show examples from the different datasets (before preprocessing). From the MB dataset we use only the NAF signal in our experiments. For this reason, we include only the NAF signal from MB in Figure 3. It is difficult to visually assess the respiratory signals and extract the domain specific features, especially since the variance of the data is very high. This is apparent in Figure 3 when trying to compare between the NAF data from AE and MB . Generally, though data from MB seem to have higher variance than the data from AE between apneic and non-apneic periods, and also higher fluctuations in the breathing pattern of the patients. Regarding the digit datasets, the differences between the datasets are more apparent. For example some obvious differences we can identify from Figure 2 are: (1) M and U are handwritten digits, whereas S are artificially made, (2) S in many cases contains additional numbers in the image, (3) digits from U seem to capture larger part of the image in relation to digits from M .

4.0.1 Devices

Finally, please note that for the sleep apnea set of experiments, the devices used are of the same type across the different datasets (AE , MB and $A3$) i.e., nasal thermistors for the NAF signal, Respiratory Inductive Plethysmography (RIP) (Chest-Abdomen belts) for the Resp A and C signals, and pulse oximeter for the measurement of oxygen saturation SpO2.

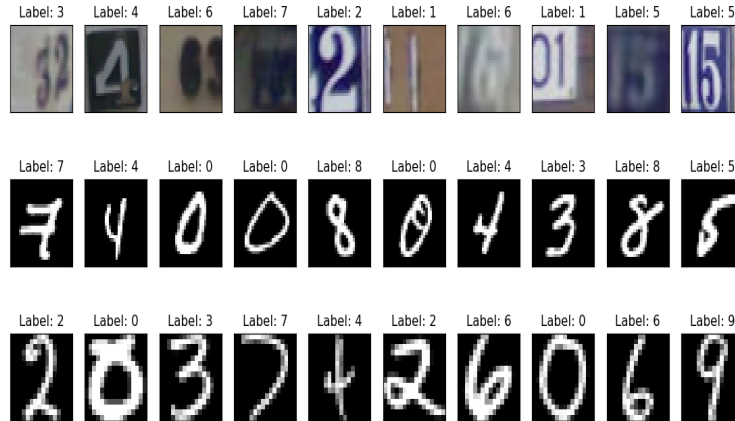


Figure 2: Examples of different datapoints from the Digit datasets: First row: examples from SVHN. Second row: examples from MNIST. Third row: examples from USPS.

4.1 Metrics

For the Digit Classification experiments, we use accuracy as performance metric since it is commonly used in related literature for the particular task, assuming a well-balanced dataset. For the apnea detection experiments, we use the kappa coefficient [17] as performance metric since it better captures performance characteristics in a single metric than accuracy, as it takes into account the possibility that two annotators (real labels and predictions in our case) agree by chance. For completion, we present the accuracy, specificity, and sensitivity results in Appendix B. All experiments are repeated for 5 iterations, and we present the average results and the standard error.

4.2 Digit Classification

We use the same architecture for all classifiers (i.e., $h_{src}, h_{CL1} \dots h_{CLn}, h_{tg}$) in all Digit classification experiments. This means that for any given instance of the algorithm we have only one model in memory. We use a convolutional neural network (CNN) with a similar but wider architecture to LeNet-5 with more weights per layer (see Table 1), and one more fully-connected layer and Convolution layers. We chose this architecture as this is a well-established simple model that is very often used for digit classification. Note that we do not use MaxPool. on the third Conv. layer for the $S \rightarrow M$, and $M \leftrightarrow U$ experiments. We use more weights to potentially compensate for the larger datasets (i.e.,

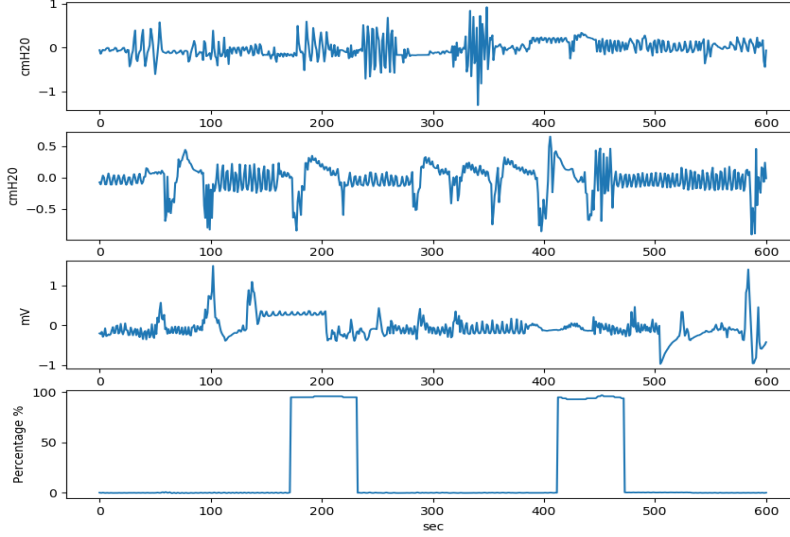


Figure 3: Different respiratory signals from *MB* and *AE*. All rows show randomly chosen 600sec windows of respiratory signals from *MB* (first row with Resp N) and *AE* (Second Row with Resp N. Third row with Resp C. and Fourth row with SpO2).

Table 1: Architectures used for the experiments (Conv: input channels \times output channels \times filter, MP: Max Pooling, fc: Fully connected, input \times output)

Architectures used			
Layers	$M \leftrightarrow U$	$S \rightarrow M$	Sl.Apnea
Conv+MP	$1 \times 32 \times 5 \times 5$	$1 \times 32 \times 5 \times 5$	$1 \times 16 \times 4$
Conv+MP	$32 \times 28 \times 5 \times 5$	$32 \times 64 \times 3 \times 3$	$16 \times 32 \times 4$
Conv(+MP)	$28 \times 28 \times 5 \times 5$	$64 \times 128 \times 5 \times 5$	$32 \times 64 \times 4$
FC	$(7 \times 7 \times 28) \times 1024$	$(7 \times 7 \times 128) \times 3072$	$(8 \times 64) \times 64$
FC	1024×128	3072×1024	64×32
out	128×10	1024×10	32×2

SVHN) and relu activations to all layers, softmax output, and dropout in the fully-connected layers. Additionally for the network of the $S \rightarrow M$ experiment we perform Batch Normalization. For all experiments, we use a batch size of 128, learning rate of 0.001, and the Adam optimizer [18]. All differences in results (mean accuracies) between h_{src} on the D_{tg} test set and h_{tg} on the D_{tg} test set are statistically significant based on the one-tailed paired t-test (for $p = 0.05$). We use this test as an indication of the importance of the improve-

ment in performance that we observe for h_{tg} compared to h_{src} on the D_{tg} test set.

We trained h_{src} for $M \rightarrow U$ and $U \rightarrow M$ for 4688 batches (i.e., 600K datapoints). For $S \rightarrow M$, we trained h_{src} for 7812 batches (i.e., 10^6 datapoints), since h_{src} does not converge with only 4688 batches when trained on S . When D_{tg} is either M or U we use the fixed number of datapoints criterion $C\{h\}$ as explained in Section 3.3.1, with $m = 200$ datapoints per-class to construct D_{CL0} , and $m = 100$ datapoints per-class for all subsequent D_{CLi} . The algorithm stops when we do not have any more unlabeled data in D_{tg} . For more details please refer to Appendix A.

Table 2: Accuracy of digit classification

<i>SICO</i> h_{tg} performance on digit classification DA (Accuracy)			
	$M \rightarrow U$	$U \rightarrow M$	$S \rightarrow M$
h_{src}, D_{src} :	99.12 \pm 0.01	96.62 \pm 0.16	90.55 \pm 0.40
h_{src}, D_{tg} :	79.83 \pm 0.51	69.58 \pm 2.00	65.94 \pm 1.97
h_{tg}, D_{tg} :	89.32 \pm 0.70	90.88 \pm 0.69	86.95 \pm 1.77

Table 2 presents the classification performance of the three combinations for h_{src} on D_{src} , and h_{tg} and h_{src} on D_{tg} . From Table 2 we notice that h_{tg} outperforms h_{src} for all $D_{src} \rightarrow D_{tg}$ cases. This could potentially be attributed to the use of domain specific knowledge (in the form of training data from D_{src}) to train all subsequent h_{CLi} and the h_{tg} , with a given confidence defined by the used criterion. Notice the steep drop of h_{src} in all cases from D_{src} to D_{tg} , which are expected due to the domain differences. We notice the largest drop for the case of $S \rightarrow M$ (24.61%). The largest improvement is observed again for the case of $S \rightarrow M$ (21.01%).

4.3 Sleep Apnea Detection

To perform sleep apnea DA, we use again identical architectures for all classifiers, i.e., $h_{src}, h_{CL1} \dots h_{CLn}, h_{tg}$. We use a 1D CNN (see Table 1), and use relu activations, dropout on the fully connected layers, and softmax activations on the output. When the A3 study is D_{src} , we train h_{src} for 15 epochs and when MB , or AE are D_{src} we train h_{src} for 20 epochs (in order to have more training iterations since MB and AE are smaller than $A3$). We use in all experiments a batch size of 128, learning rate of 0.001, and the Adam optimizer [18]. Note that all differences in results between h_{src} on the D_{tg} test set and h_{tg} on the D_{tg} test set are statistically significant based on the one-tailed paired t-test (for $p = 0.05$), with the exception of Resp A: $A3 \rightarrow AE$, NAF: $A3 \rightarrow MB$, and Resp C: $AE \rightarrow A3$.

We use in all experiments with *AE* and *MB* as D_{tg} the fixed data criterion with 500 datapoints per-class for h_{src} and 200 datapoints per class for all subsequent h_{CLi} as belief criterion. With *A3* as D_{tg} , we use the fixed data criterion with 10000 datapoints per-class for h_{src} and 500 datapoints per class for all subsequent h_{CLi} , since *A3* is much larger. The algorithm stops when we do not have any more unlabeled data in D_{tg} .

Table 3: Performance for DA between different dataset combinations for the NAF sensor signal.

<i>SICO</i> h_{tg} performance (kappa $\times 100$) for NAF			
NAF:	h_{src}, D_{src}	h_{src}, D_{tg}	h_{tg}, D_{tg}
<i>A3</i> \rightarrow <i>AE</i> :	69.33 \pm 0.21	67.46 \pm 5.38	84.07 \pm 4.76
<i>A3</i> \rightarrow <i>MB</i> :	69.33 \pm 0.21	10.26 \pm 1.13	19.30 \pm 1.78
<i>AE</i> \rightarrow <i>MB</i> :	94.39 \pm 0.49	11.96 \pm 1.15	13.14 \pm 0.63
<i>MB</i> \rightarrow <i>AE</i> :	41.69 \pm 1.60	65.27 \pm 3.03	78.88 \pm 2.25
<i>AE</i> \rightarrow <i>A3</i> :	94.39 \pm 0.49	29.67 \pm 1.09	36.68 \pm 2.60

Table 3 presents the classification performance of the three combinations for h_{src} on D_{src} and h_{tg} and h_{src} on D_{tg} . From Table 3 we initially notice the significant impact of the quality of the datasets on the performance of h_{src} . For *MB* \rightarrow *AE*, the quality of the *MB* data is low enough that the evaluation of h_{src} on the test set of *MB* performs worse than the evaluation of h_{src} in *AE*. Since *AE* is a high quality dataset, it is easier to have much better performance. This is reflected by the very big difference of kappa ($\times 100$) between the two datasets for h_{src} (i.e., 41.69 vs. 94.39). For *A3*, we expected that it would have better transferability to the other datasets since it is much larger, thus covering a wider variety of cases (both from a patient and from a data quality perspective). Though this holds for the *AE* case, i.e., *A3* \rightarrow *AE*, it is not the case for *MB*, for which (*A3* \rightarrow *MB*) h_{src} performs very poorly. It is noteworthy however that we get significantly better results with *SICO* for *A3* \rightarrow *MB* than for *AE* \rightarrow *MB*. In summary, we identify D_{src} ’s data quality and variation as two important factors which affect the performance of h_{src} and h_{tg} for D_{tg} .

Generally, h_{tg} performs for all cases better than h_{src} on D_{tg} . As expected from Eq. 2.2, h_{src} plays a very critical role in the *SICO* process, and we cannot get very good results if the performance of h_{src} is initially very low. We discuss this characteristic in more detail in Section 5. Finally, another noteworthy observation is the very large standard error for all cases for h_{src} on D_{tg} , and to a lesser extent for *SICO*. The results for h_{src} were not stable among the different iterations of the experiment (for example for *A3* \rightarrow *AE* the range of kappa $\times 100$ values was 54.3-81.9). However h_{tg} , consistently outperformed h_{src} , and it additionally provided a stabilizing effect, as the results for h_{tg} did not vary as much (with the exception of *AE* \rightarrow *A3*).

4.3.1 Other Sensors

We repeat the experiment for the $A3 \rightarrow AE$ combination for the additional respiratory sensors which are included in $A3$ and AE , i.e., Abdominal Respiration (Resp A), Oxygen Saturation (Sp02) and Chest Respiration (Resp C). We do not use MB for these experiments due to the small number of recordings per-sensor and the already very low performance it yields for all experiments even with the NAF signal, for which we have much more data in comparison to the other signals. The other parameters are the same as in the previous experiments.

Table 4: Performance of $A3 \rightarrow AE$ and $AE \rightarrow A3$ for Resp A, Sp02, and Resp C

<i>SICO</i> h_{tg} Performance ($\kappa \times 100$) for different sensors			
	Resp A	Resp C	Sp02
$A3 \rightarrow AE: h_{src}, D_{src}$:	66.74 \pm 0.38	66.91 \pm 0.30	71.84 \pm 0.67
$A3 \rightarrow AE: h_{src}, D_{tg}$:	78.95 \pm 1.92	57.23 \pm 8.38	61.23 \pm 4.44
$A3 \rightarrow AE: h_{tg}, D_{tg}$:	80.68 \pm 0.84	81.47 \pm 1.12	74.23 \pm 2.07
$AE \rightarrow A3: h_{src}, D_{src}$:	92.31 \pm 0.50	90.97 \pm 0.45	88.93 \pm 0.36
$AE \rightarrow A3: h_{src}, D_{tg}$:	27.35 \pm 1.04	23.07 \pm 1.89	-0.32 \pm 0.00
$AE \rightarrow A3: h_{tg}, D_{tg}$:	48.47 \pm 1.20	26.00 \pm 0.53	19.37 \pm 1.58

The results are found in Table 6. We notice that h_{tg} significantly outperforms h_{src} on D_{tg} (with the exception of Resp A). As before, we have with $A3 \rightarrow AE$ a very large standard error (big variation) for h_{src} , and *SICO* seems to have a stabilizing effect on the variation. For these experiments, this phenomenon is more pronounced than for the Resp N. experiment. Again, we observe for Resp A: $A3 \rightarrow AE$ the same interesting pattern that we observed for NAF: $MB \rightarrow AE$, i.e., that h_{src} has a higher performance on the target test set than the source test set. We hypothesize that this happens for similar reasons as before, i.e., due to the better quality and potential homogeneity of AE relative to $A3$. This hypothesis is strengthened by the fact that for the $A3 \rightarrow AE$ adaptation all sensor signals seem to perform relatively well (with the exception of Resp C). Another interesting characteristic is that Sp02 which has the best performance for $A3$, seems to adapt much worse to the new domain, i.e., AE , than Resp A.

In the $AE \rightarrow A3$ experiments h_{tg} outperforms h_{src} again for all cases. However, this time the variation for h_{src} in D_{src} is smaller than for h_{tg} . This could potentially again be attributed to the larger data variety in the $A3$, which can make DA more stable regardless of the initialization, and training randomness for h_{src} . Interestingly, h_{src} has seemingly not generalized in the Resp Sp02 experiments. Intuitively, this leads us to assume that h_{tg} should also fail. However, the results show that to some extent that h_{tg} is still able to learn. For a h_{src} trained with AE on Sp02 and tested on $A3$ Sp02, we observe that for the train set, the specificity between the pseudo-labels and the true labels is 0.952

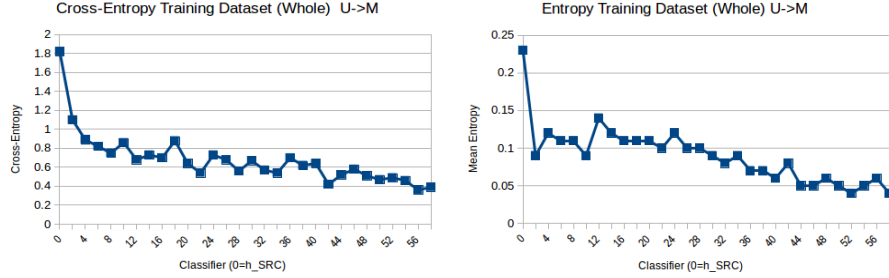


Figure 4: Mean cross-entropy loss with the real labels, (a) and Mean entropy (b) for the whole target training dataset.

and sensitivity is 0.08. For the same h_{src} , for D_{CL0} , specificity is 0.67, sensitivity 0.33. We notice that we achieve already with the first h_{CL1} a kappa ($\times 100$) value of 16. We hypothesize, that the performance improvement occurs due to the recognition from h_{CL1} of unique characteristics of each class. This could be a result of the better balancing between the correct data from each class, together with the potentially uninformative nature of the wrong class data. Due to this uninformative nature, h_{CL1} does not generalize as much towards a wrong pattern. Intuitively, this means that h_{src} learned a useful structure of the feature space for both classes. Due to the better balancing of D_{CL0} , the "hidden" structure learned for the minority class is uncovered for the classifier trained on D_{CL0} , i.e., h_{CL1} , allowing it to generalize better to new data.

4.4 Training Analysis

In *SICO*, we train sequentially n classifiers, each one to a high-confidence sub-region of the training dataset, which is a superset of the region that the previous classifier has been trained. Thus, assuming that the accumulative error $\Delta_i(h_{tg}; h_{src}, h_{CL1} \dots h_{CL(i-1)})$ for every classifier h_{CLi} in the sequence does not get too large, we expect that the cross-entropy loss with the true training labels will become smaller, because each classifier learns with an expanding amount of datapoints from the training dataset.

Figure 4 (a) presents the training dataset cross-entropy loss for $U \rightarrow M$, for $m = 500$ per-class for h_{src} and $m = 200$ per-class for the subsequent h_{CLi} , based on the fixed number of datapoints criterion. As expected, the loss decreases as the datasets D_{CLi} become larger and the algorithm proceeds. This is mapped also in the performance on new data as shown in Figure 5 (a), which depicts the test set performance in terms of accuracy of M for all different h_{CLi} . In this Figure, we also include the performance of the test set of U (orange) for completion. The performance of U is as expected degrading as the algorithm proceeds.

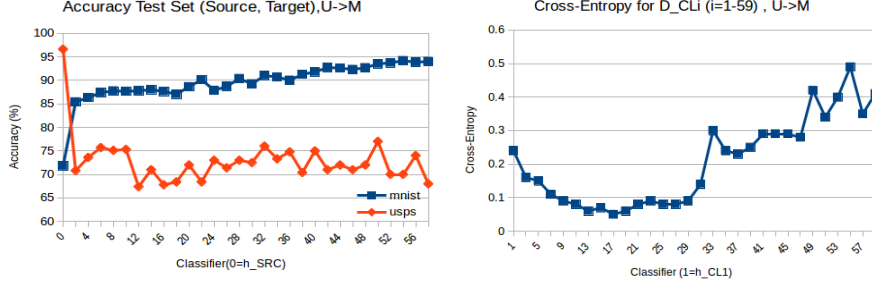


Figure 5: Test accuracy (hypothetical) for all h_{CLi} , (a). Mean cross-entropy loss for each dataset $D_{CL(i-1)}$ for the respective h_{CLi} , (b). We show the results for every second classifier h_{CLi} (dots) for better readability. All figures were obtained on the same run.

Additionally, Figure 5 (b) shows the mean cross-entropy with the real labels for D_{CLi} for all i . Notice that the error initially becomes smaller, which means that the new regions that are included in D_{CLi} to form $D_{CL(i+1)}$ yield better performance than the previous i . However, after some iterations this does not hold, and the performance with the new $D_{CL(i+1)}$ degrades in relation to D_{CLi} . This means that the mean Δ_i becomes larger. We hypothesize that this behavior could be attributed to the misalignment between the left out data that later iterations represent and the initial high confidence region of h_{src} .

We expect that for increasing values of i the average entropy of h_{CLi} becomes smaller. Since each new h_{CLi} uses a larger part of D_{tg} and trains on hard labels from $h_{CL(i-1)}$, it will be more "confident" for a larger part of D_{tg} . Figure 4 (b) showcases this phenomenon. Furthermore, h_{CLi} has been trained with more data and thus can potentially generalize better to new data.

5 Discussion

From the above evaluation, we observe that the success of *SICO* on D_{tg} depends on how well the initial h_{src} can generalize on D_{tg} . This observation occurs directly from Eq. 2.2, since the error of h_{src} , recursively propagates for all Δ_i which constitute the total Δ_n . Thus, if h_{src} does not perform well on D_{tg} this has a direct repeated negative impact on the whole *SICO* algorithm. Interestingly however, even for the cases for which h_{src} performs really bad on D_{tg} (mainly for the cases which include *MB* and *A3* as D_{tg}) h_{tg} is still able to outperform h_{src} . This potentially happens due to the fact that we expect better performance for high-confidence regions than the average performance, assuming that we trust h_{src} adequately. This means that a smaller error propagates through the algorithm, than for the case in which we have a lower confidence region. This insight is one of the main inspirations for this work.

However, if we use too few data points as our confidence region, then the classifier trained on this region will not be able to generalize well enough to new data, and will have higher generalization error for the new regions. Thus, there exist a trade-off between confidence and trust on the one hand, and generalization capability on the other hand. This needs to be taken into account to determine how strict the criterion $C\{h\}$ should be, as this decides how many datapoints a new D_{CLi} will have.

Finally, a natural extension to the proposed approach is to apply probabilistically the criterion C that we use, instead of using it as a hard threshold of acceptance for a given datapoint. As this is a more natural approach that better captures the probabilistic nature of density estimation that the classifiers perform, we hypothesize that it can yield even better results than the original hard acceptance/rejection method. However, in preliminary experiments we were not able to showcase improvement in performance in relation to the original method.

5.0.1 Implications for Detecting a Condition at the End-User

The proposed approach provides a way for a trained classifier to adapt to a new domain. In the context of healthcare, one application could regard adaptation between different patients. For example, for the OSA case, if we have a person whose datapoints (i.e., one-minute windows) are different due to a variety of potential factors than the datapoints h_{src} has been trained with, we can expect that by applying *SICO* we can get a better performing classifier for the particular individual. Additionally, assuming that we apply the criterion C , we can properly adapt in a dataset which is balanced with different class frequencies in relation to the source dataset. This, in the context of condition detection means that we could potentially adapt from patients who do not have many pathological datapoints to patients for which the condition is more expressed.

6 Related Work

There is a large body of work in DA, mainly focused on the visual domain, which is to a large extent covered by existing surveys [19, 20]. In one of these surveys [20] Wang et al. separate domain adaptation based on the type of learning (supervised, semi-supervised, unsupervised), whether or not the feature space is the same in source and target domains, and whether the work performs one-step or multi-step DA. We follow a similar separation, however due to space limitations we focus on the works that are mostly related to ours. Thus, we separate on the basis of supervised or unsupervised DA, with more emphasis on unsupervised DA, and for the unsupervised DA case whether the proposed work has direct or indirect access to the source data (see Figure 6). Furthermore, we separate for visual and time-series applications or methods. For the works which resemble our work, we compare and discuss about specific similarities and differences.

For the case of unsupervised visual DA, a large body of literature use vari-

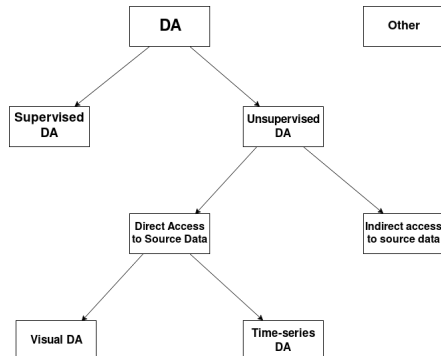


Figure 6: Classification of presented related works in supervised or unsupervised DA.

ations of adversarial domain adaptation for visual applications [21, 22, 23, 24, 25, 26]. A good example of an advanced technique that also includes adversarial elements is CyCADA [27]. It is a technique for unsupervised DA which uses a team of models trained on a unified loss which consists of task losses, cycle-consistent loss [28], GAN losses and semantic consistency loss. The goal is to adapt representations at pixel and feature level while enforcing cycle and semantic consistency loss. Other works for visual applications that do not directly include adversarial training include [29, 30]. Additionally, works exist which, like our proposed method, make use of pseudo-labelling on the target domain [31, 32, 33, 34]. However, all of these approaches take advantage of both source and target domain data during their training phase. Furthermore, they use different methods for classifier adaptation on the conditional distribution of the target domain during their training phase, like entropy minimization, minimization of the conditional distribution’s MMD between source and target, pseudo-labelling with multiple classifiers etc.

As mentioned, most of the above techniques perform unsupervised DA with access to labeled source data and unlabeled target data. However, we focus on DA at the end-user with access only to unlabeled target’s data and a trained classifier at the source data and labels, making it an inherently harder problem (see Figure 6 Unsupervised DA right leaf). Despite these additional restrictions, *SICO* yields an on-average comparable or superior performance relative to several other well-established unsupervised DA works for the digit datasets (for example the results reported in [23, 35]). Additional works that provide a solution to unsupervised DA without direct access to the labeled source data include [36, 37]. Wulfmeier et al. [36] address the problem of degraded model performance due to continuously shifting environment conditions. They develop incremental adversarial DA with which they redefine DA as a stream of incrementally changing domains, to enable a classifier to adapt for example to changing weather conditions, day night circle, etc. Additionally, they propose an extension to use only target data assuming an additional GAN generator

which has learned the encoded feature marginal distribution of the source data. Similarly, our method uses the source data indirectly via h_{src} . However, we investigate the normal domain adaptation scenario, and not a case of transitioning incremental domain shifts. Li et al. [37] introduce Adaptive Batch Normalization (AdaBN), and use only a classifier and the target data. They standardize each neuron’s output with the average and standard deviation of its output from the images in the target domain. This standardization ensures that each neuron receives data from a similar distribution, no matter of which domain the data come from. Using this idea, Zhang et al. [38], train a convolutional network with layers of various kernel sizes for fault diagnosis on raw vibration signals. They then perform AdaBN for the CNN model trained in the source domain. However, this approach does not train with the target domain data, and is only a form of cross domain normalization for the trained classifier. As a result we hypothesize that it does not take full advantage of the knowledge potential of the target sample.

For the case of unsupervised DA for time-series data, Purushotham et al. [39], use Variational Recurrent Neural Nets [40], and employ adversarial DA to train in order to achieve DA from the latent representations. In [41], Aswolinskiy et al., propose Unsupervised Transfer Learning via Self-Predictive Modelling. In the proposed approach, a linear transformation Q is learned that minimizes the error identified by a self-predictive model between the source and the transformed by Q target domain. Then a classifier trained in the source domain is applied in the transformed target domain. We assigned this work under the umbrella of unsupervised domain adaptation since, as mentioned in the paper, the authors present a general domain adaptation framework and because it fits the data access criteria we specify. Other works include [42, 43, 38]. Chai et al. [42] perform EEG domain adaptation for sentiment recognition by using a linear transformation function that matches the marginal distributions of the source and target feature spaces. They additionally employ a pseudo-labelling approach to transfer confident target data to the transformed source domain which relates to our own approach for choosing confident samples. Natarajaan et al. [43] use DA in order to mitigate the negative effects from the lab-to-field transition for cocaine detection using wearable ECG.

In the context of supervised DA, Persello et al. [44, 45], use Active Learning for DA for classification of remote sensing images. This approach loosely relates to ours, in the sense that it iteratively trains the classifier with a differentiating training set. However, the proposed approach assumes access to the source data (for data points to be removed from the training set), and a user in the role of supervisor, which assigns labels for chosen samples.

Finally, other works that are related in the context of our work include [46, 47, 48]. Fawaz et al. [46] use transfer learning for time series classification. They evaluate on the UCR archive for all possible combinations, and use a method that relies on Dynamic Time Warping to measure the similarity between the different datasets. Regarding CL, both works included apply DA in the context of semantic segmentation. Zou et al. [47] utilize pseudolabels and self-training to learn the new domain. Contrary to our work, they use a loss

which contains terms for the loss of the source and the target domain plus a L_1 -regularization term on the pseudolabels. They optimize in a two-step fashion, optimizing first the pseudolabels and then the classifier weights. Zhang et al. [48] derive their curriculum by separating between the hard task of semantic segmentation from the easy task of learning high-level properties of the unknown labels. They minimize a joint loss which includes terms from both domains. For their easy task they infer the target labels and landmark pixel labels by utilizing training and labelling in the source domain (e.g, retrieving the nearest source neighbors for a target image and transfer the labelling).

7 Conclusion

The primary motivation for our work is to enable end-users to create personal classifiers, e.g., for health applications without labeled data. In particular, we foresee a collaboration in which a host releases a classifier h_{src} , and the end-user (a patient in our case), uses her data and the classifier to create a new personalized classifier (i.e., adapted to the domain of the end-user). In this work we achieve this by performing *SICO*. *SICO*, iteratively adapts classifiers to the new domain based on high-confidence data from the previous classifiers, and without the need of the source data and labels. Based on our scenario, we are more interested in the case of performing DA at the end-user, but obviously *SICO* can also be applied at the host. We apply *SICO* for the case of sleep apnea detection, and use a large real-world clinical dataset for its evaluation. Additionally, we experiment with two open sleep monitoring datasets and the MNIST, SVHN and USPS datasets for digit classification. By this, we achieve (1) reproducibility, (2) demonstrate the generalizability of *SICO* for another task, and (3) achieve comparability with related work. The results from these experiments show consistently better performance of h_{tg} in comparison to h_{src} , as expected. Depending on the case, we get an increase in kappa of up to 0.24. For the task of digit classification DA, *SICO* achieves again a consistently good performance. Despite the additional limitations of the scenario that we investigate, the performance of several well established related works e.g., ADDA and gradient reversal is lower than the presented results of this paper.

As a next step, we are interested in investigating how well can the technique be applied if the source classifier is trained under differential privacy guarantees. Another interesting application we investigate is the combination of the proposed approach with a style transfer method with the goal of increasing the DA capabilities of the approach for tasks containing different types of sensors.

Acknowledgements

This work was performed as part of the CESAR project (nr. 250239/O70) funded by The Research Council of Norway.

References

- [1] Sinno Jialin Pan and Qiang Yang. A survey on transfer learning. *IEEE Transactions on knowledge and data engineering*, 22(10):1345–1359, 2009.
- [2] Yaroslav Ganin and Victor Lempitsky. Unsupervised domain adaptation by backpropagation. *arXiv preprint arXiv:1409.7495*, 2014.
- [3] Guoliang Kang, Lu Jiang, Yi Yang, and Alexander G Hauptmann. Contrastive adaptation network for unsupervised domain adaptation. In *Proceedings of the IEEE Conference on Computer Vision and Pattern Recognition*, pages 4893–4902, 2019.
- [4] Stein Kristiansen, Mari Sønsteby Hugaas, Vera Goebel, Thomas Plagemann, Konstantinos Nikolaidis, and Knut Liestøl. Data mining for patient friendly apnea detection. *IEEE Access*, 6:74598–74615, 2018.
- [5] Konstantinos Nikolaidis, Stein Kristiansen, Vera Goebel, Thomas Plagemann, Knut Liestøl, and Mohan Kankanhalli. Augmenting physiological time series data: A case study for sleep apnea detection. *arXiv preprint arXiv:1905.09068*, 2019.
- [6] Baile Xie and Hlaing Minn. Real-time sleep apnea detection by classifier combination. *IEEE Transactions on information technology in biomedicine*, 16(3):469–477, 2012.
- [7] Matt Fredrikson, Somesh Jha, and Thomas Ristenpart. Model inversion attacks that exploit confidence information and basic countermeasures. In *Proceedings of the 22Nd ACM SIGSAC Conference on Computer and Communications Security, CCS ’15*, pages 1322–1333, New York, NY, USA, 2015. ACM.
- [8] Shai Ben-David, John Blitzer, Koby Crammer, and Fernando Pereira. Analysis of representations for domain adaptation. In *Advances in neural information processing systems*, pages 137–144, 2007.
- [9] Yoshua Bengio, Jérôme Louradour, Ronan Collobert, and Jason Weston. Curriculum learning. In *Proceedings of the 26th annual international conference on machine learning*, pages 41–48, 2009.
- [10] Guy Hacohen and Daphna Weinshall. On the power of curriculum learning in training deep networks. *arXiv preprint arXiv:1904.03626*, 2019.
- [11] Yann LeCun, Léon Bottou, Yoshua Bengio, and Patrick Haffner. Gradient-based learning applied to document recognition. *Proceedings of the IEEE*, 86(11):2278–2324, 1998.
- [12] Jonathan J. Hull. A database for handwritten text recognition research. *IEEE Transactions on pattern analysis and machine intelligence*, 16(5):550–554, 1994.

- [13] Yuval Netzer, Tao Wang, Adam Coates, Alessandro Bissacco, Bo Wu, and Andrew Y Ng. Reading digits in natural images with unsupervised feature learning. 2011.
- [14] Thomas Penzel, George B Moody, Roger G Mark, Ary L Goldberger, and J Hermann Peter. The apnea-ecg database. In *Computers in Cardiology 2000. Vol. 27 (Cat. 00CH37163)*, pages 255–258. IEEE, 2000.
- [15] Yuhei Ichimaru and GB Moody. Development of the polysomnographic database on cd-rom. *Psychiatry and clinical neurosciences*, 53(2):175–177, 1999.
- [16] Gunn Marit Traaen, Lars Aakerøy, et al. Treatment of sleep apnea in patients with paroxysmal atrial fibrillation: Design and rationale of a randomized controlled trial. *Scandinavian Cardiovascular Journal*, (52:6,pp. 372-377):1–20, January 2019.
- [17] Jacob Cohen. A coefficient of agreement for nominal scales. *Educational and psychological measurement*, 20(1):37–46, 1960.
- [18] Diederik P Kingma and Jimmy Ba. Adam: A method for stochastic optimization. *arXiv preprint arXiv:1412.6980*, 2014.
- [19] Gabriela Csurka. Domain adaptation for visual applications: A comprehensive survey. *arXiv preprint arXiv:1702.05374*, 2017.
- [20] Mei Wang and Weihong Deng. Deep visual domain adaptation: A survey. *Neurocomputing*, 312:135–153, 2018.
- [21] Mingsheng Long, Zhangjie Cao, Jianmin Wang, and Michael I Jordan. Conditional adversarial domain adaptation. In *Advances in Neural Information Processing Systems*, pages 1640–1650, 2018.
- [22] Eric Tzeng, Judy Hoffman, Kate Saenko, and Trevor Darrell. Adversarial discriminative domain adaptation. In *The IEEE Conference on Computer Vision and Pattern Recognition (CVPR)*, July 2017.
- [23] Yaroslav Ganin, Evgeniya Ustinova, Hana Ajakan, Pascal Germain, Hugo Larochelle, François Laviolette, Mario Marchand, and Victor Lempitsky. Domain-adversarial training of neural networks. *The Journal of Machine Learning Research*, 17(1):2096–2030, 2016.
- [24] Ming-Yu Liu, Thomas Breuel, and Jan Kautz. Unsupervised image-to-image translation networks. In *Advances in neural information processing systems*, pages 700–708, 2017.
- [25] Mingsheng Long, Han Zhu, Jianmin Wang, and Michael I Jordan. Deep transfer learning with joint adaptation networks. In *Proceedings of the 34th International Conference on Machine Learning-Volume 70*, pages 2208–2217. JMLR. org, 2017.

- [26] Ming-Yu Liu and Oncel Tuzel. Coupled generative adversarial networks. In *Advances in neural information processing systems*, pages 469–477, 2016.
- [27] Judy Hoffman, Eric Tzeng, Taesung Park, Jun-Yan Zhu, Phillip Isola, Kate Saenko, Alexei A Efros, and Trevor Darrell. Cycada: Cycle-consistent adversarial domain adaptation. *arXiv preprint arXiv:1711.03213*, 2017.
- [28] Jun-Yan Zhu, Taesung Park, Phillip Isola, and Alexei A. Efros. Unpaired image-to-image translation using cycle-consistent adversarial networks. In *The IEEE International Conference on Computer Vision (ICCV)*, Oct 2017.
- [29] Konstantinos Bousmalis, George Trigeorgis, Nathan Silberman, Dilip Krishnan, and Dumitru Erhan. Domain separation networks. In *Advances in neural information processing systems*, pages 343–351, 2016.
- [30] Philip Haeusser, Thomas Frerix, Alexander Mordvintsev, and Daniel Cremers. Associative domain adaptation. In *The IEEE International Conference on Computer Vision (ICCV)*, Oct 2017.
- [31] Hongliang Yan, Yukang Ding, Peihua Li, Qilong Wang, Yong Xu, and Wangmeng Zuo. Mind the class weight bias: Weighted maximum mean discrepancy for unsupervised domain adaptation. In *The IEEE Conference on Computer Vision and Pattern Recognition (CVPR)*, July 2017.
- [32] Xu Zhang, Felix Xinnan Yu, Shih-Fu Chang, and Shengjin Wang. Deep transfer network: Unsupervised domain adaptation. *arXiv preprint arXiv:1503.00591*, 2015.
- [33] Kuniaki Saito, Yoshitaka Ushiku, and Tatsuya Harada. Asymmetric tri-training for unsupervised domain adaptation. In *Proceedings of the 34th International Conference on Machine Learning-Volume 70*, pages 2988–2997. JMLR. org, 2017.
- [34] Mingsheng Long, Han Zhu, Jianmin Wang, and Michael I Jordan. Unsupervised domain adaptation with residual transfer networks. In D. D. Lee, M. Sugiyama, U. V. Luxburg, I. Guyon, and R. Garnett, editors, *Advances in Neural Information Processing Systems 29*, pages 136–144. Curran Associates, Inc., 2016.
- [35] Eric Tzeng, Judy Hoffman, Kate Saenko, and Trevor Darrell. Adversarial discriminative domain adaptation. In *Proceedings of the IEEE Conference on Computer Vision and Pattern Recognition*, pages 7167–7176, 2017.
- [36] Markus Wulfmeier, Alex Bewley, and Ingmar Posner. Incremental adversarial domain adaptation for continually changing environments. In *2018 IEEE International conference on robotics and automation (ICRA)*, pages 1–9. IEEE, 2018.

- [37] Yanghao Li, Naiyan Wang, Jianping Shi, Jiaying Liu, and Xiaodi Hou. Revisiting batch normalization for practical domain adaptation. *arXiv preprint arXiv:1603.04779*, 2016.
- [38] Wei Zhang, Gaoliang Peng, Chuanhao Li, Yuanhang Chen, and Zhujun Zhang. A new deep learning model for fault diagnosis with good anti-noise and domain adaptation ability on raw vibration signals. *Sensors*, 17(2):425, 2017.
- [39] Sanjay Purushotham, Wilka Carvalho, Tanachat Nilanon, and Yan Liu. Variational recurrent adversarial deep domain adaptation. 2016.
- [40] Junyoung Chung, Kyle Kastner, Laurent Dinh, Kratarth Goel, Aaron C Courville, and Yoshua Bengio. A recurrent latent variable model for sequential data. In *Advances in neural information processing systems*, pages 2980–2988, 2015.
- [41] Witali Aswolinskiy and Barbara Hammer. Unsupervised transfer learning for time series via self-predictive modelling-first results. In *Proceedings of the Workshop on New Challenges in Neural Computation (NC2)*, volume 3, 2017.
- [42] Xin Chai, Qisong Wang, Yongping Zhao, Yongqiang Li, Dan Liu, Xin Liu, and Ou Bai. A fast, efficient domain adaptation technique for cross-domain electroencephalography (eeg)-based emotion recognition. *Sensors*, 17(5):1014, 2017.
- [43] Annamalai Natarajan, Gustavo Angarita, Edward Gaiser, Robert Malison, Deepak Ganesan, and Benjamin M Marlin. Domain adaptation methods for improving lab-to-field generalization of cocaine detection using wearable eeg. In *Proceedings of the 2016 ACM International Joint Conference on Pervasive and Ubiquitous Computing*, pages 875–885. ACM, 2016.
- [44] Claudio Persello and Lorenzo Bruzzone. Active learning for domain adaptation in the supervised classification of remote sensing images. *IEEE Transactions on Geoscience and Remote Sensing*, 50(11):4468–4483, 2012.
- [45] Claudio Persello. Interactive domain adaptation for the classification of remote sensing images using active learning. *IEEE geoscience and remote sensing letters*, 10(4):736–740, 2012.
- [46] Hassan Ismail Fawaz, Germain Forestier, Jonathan Weber, Lhassane Idoumghar, and Pierre-Alain Muller. Transfer learning for time series classification. In *2018 IEEE International Conference on Big Data (Big Data)*, pages 1367–1376. IEEE, 2018.
- [47] Yang Zou, Zhiding Yu, BVK Vijaya Kumar, and Jinsong Wang. Unsupervised domain adaptation for semantic segmentation via class-balanced self-training. In *Proceedings of the European conference on computer vision (ECCV)*, pages 289–305, 2018.

- [48] Yang Zhang, Philip David, and Boqing Gong. Curriculum domain adaptation for semantic segmentation of urban scenes. In *Proceedings of the IEEE International Conference on Computer Vision*, pages 2020–2030, 2017.

A Additional Design Decisions

In this Appendix, we discuss additional design decisions made during the algorithm.

- **Use of hard or soft labels for labelling of $D_{CLi}, i = 0..N$:** In the original approach we use as labels the one-hot encoding vector based on the maximum argument of the output class probabilities of the classifier which is doing the labelling for the particular datapoint. Thus each new classifier is trained on one-hot encoding labels. Alternatively, we can utilize directly the output class probabilities to act as labels and for the training of each new classifier. During our experiments, we experimented with this approach, however in almost all cases it yielded worst results than the use of hard labels. As a result we use hard labelling in our final experiments. The only exception is the *MB* dataset, for which we hypothesize that due to the poor labelling quality, there is a stronger discrepancy between the true conditional distribution, and the hard labelling. This would also result in the optimal (Bayes) classifier having a very high true risk because of the poor labelling. Thus since we have a finite amount of data, using hard labels could be misrepresentative of the previous classifiers' class probabilities.
- **Training Iterations for h_{CLi} :** Depending on the sizes of the different datasets we train for a minimum of 10 (*A3*) epochs to a maximum of 50 epochs (*MB*, *AE*).

B Accuracy, Specificity, Sensitivity for Apnea Detection Experiments

Appendix B shows the Accuracy, Sensitivity and Specificity for the Apnea detection experiments DA experiments.

A characteristic which was not identifiable from the kappa values is the positive balancing effect that *SICO* has between specificity and sensitivity. When using h_{src} , notice that in many cases we obtain high specificity at the expense of high sensitivity (e.g., $NAF:A3 \rightarrow MB$, $NAF:AE \rightarrow MB$). We observe that for h_{tg} this effect is minimized. This means that h_{tg} obtains increased sensitivity compared to h_{src} . This is a positive characteristic since sensitivity (i.e., the percentage of the correctly detected apneic minutes) plays a crucial role in the context of sleep apnea detection as low sensitivity can lead to a falsely negative diagnosis, making the system inherently untrustworthy.

Table 5:

<i>SICO</i> h_{tg} Accuracy for NAF			
NAF:	h_{src}, D_{src}	h_{src}, D_{tg}	h_{tg}, D_{tg}
$A3 \rightarrow AE$:	84.75 \pm 0.11	84.37 \pm 5.62	92.16 \pm 2.18
$A3 \rightarrow MB$:	84.75 \pm 0.11	54.72 \pm 0.58	59.56 \pm 0.89
$AE \rightarrow MB$:	97.32 \pm 0.24	55.88 \pm 0.57	56.60 \pm 0.33
$MB \rightarrow AE$:	70.88 \pm 0.79	82.90 \pm 1.54	89.60 \pm 1.13
$AE \rightarrow A3$:	97.32 \pm 0.24	64.43 \pm 0.64	68.71 \pm 1.00
<i>SICO</i> h_{tg} Sensitivity for NAF			
NAF:	h_{src}, D_{src}	h_{src}, D_{tg}	h_{tg}, D_{tg}
$A3 \rightarrow AE$:	85.82 \pm 0.78	77.82 \pm 0.50	94.99 \pm 1.54
$A3 \rightarrow MB$:	85.82 \pm 0.66	26.29 \pm 2.48	52.12 \pm 3.54
$AE \rightarrow MB$:	96.08 \pm 0.24	48.50 \pm 0.74	58.34 \pm 1.77
$MB \rightarrow AE$:	73.38 \pm 0.87	86.66 \pm 2.23	95.19 \pm 0.76
$AE \rightarrow A3$:	96.08 \pm 0.24	56.78 \pm 2.32	74.32 \pm 0.96
<i>SICO</i> h_{tg} Specificity for NAF			
NAF:	h_{src}, D_{src}	h_{src}, D_{tg}	h_{tg}, D_{tg}
$A3 \rightarrow AE$:	83.50 \pm 0.73	88.93 \pm 4.59	90.29 \pm 4.24
$A3 \rightarrow MB$:	83.50 \pm 0.73	84.06 \pm 1.95	67.23 \pm 3.71
$AE \rightarrow MB$:	98.13 \pm 0.31	63.49 \pm 1.16	54.79 \pm 1.37
$MB \rightarrow AE$:	68.28 \pm 1.76	80.42 \pm 2.29	85.92 \pm 1.55
$AE \rightarrow A3$:	98.13 \pm 0.31	73.39 \pm 1.50	62.14 \pm 1.21

Table 6:

<i>SICO</i> h_{tg} Accuracy for different sensors			
	Resp A	Resp C	Sp02
$A3 \rightarrow AE: h_{src}, D_{src}:$	83.51 \pm 1.92	83.57 \pm 0.16	85.97 \pm 0.30
$A3 \rightarrow AE: h_{src}, D_{tg}:$	89.74 \pm 0.81	77.68 \pm 4.89	80.12 \pm 2.4
$A3 \rightarrow AE: h_{tg}, D_{tg}:$	90.42 \pm 0.43	90.88 \pm 0.56	87.44 \pm 1.01
$AE \rightarrow A3: h_{src}, D_{src}:$	96.32 \pm 0.24	95.66 \pm 0.02	94.76 \pm 0.17
$AE \rightarrow A3: h_{src}, D_{tg}:$	61.79 \pm 0.59	59.49 \pm 1.08	47.32 \pm 1.26
$AE \rightarrow A3: h_{tg}, D_{tg}:$	74.44 \pm 0.58	63.20 \pm 0.23	60.34 \pm 0.78
<i>SICO</i> h_{tg} Sensitivity for different sensors			
	Resp A	Resp C	Sp02
$A3 \rightarrow AE: h_{src}, D_{src}:$	86.3 \pm 0.51	85.22 \pm 0.66	85.40 \pm 1.05
$A3 \rightarrow AE: h_{src}, D_{tg}:$	93.83 \pm 5.15	92.16 \pm 4.44	94.64 \pm 0.53
$A3 \rightarrow AE: h_{tg}, D_{tg}:$	98.48 \pm 0.07	96.91 \pm 0.75	89.44 \pm 0.79
$AE \rightarrow A3: h_{src}, D_{src}:$	95.85 \pm 0.43	97.46 \pm 0.52	97.48 \pm 0.13
$AE \rightarrow A3: h_{src}, D_{tg}:$	30.76 \pm 1.27	27.92 \pm 2.39	9.53 \pm 1.29
$AE \rightarrow A3: h_{tg}, D_{tg}:$	77.46 \pm 0.54	65.51 \pm 0.70	69.16 \pm 0.97
<i>SICO</i> h_{tg} Specificity for different sensors			
	Resp A	Resp C	Sp02
$A3 \rightarrow AE: h_{src}, D_{src}:$	80.55 \pm 0.60	81.63 \pm 0.46	86.63 \pm 1.86
$A3 \rightarrow AE: h_{src}, D_{tg}:$	87.04 \pm 2.56	68.17 \pm 9.66	70.59 \pm 3.69
$A3 \rightarrow AE: h_{tg}, D_{tg}:$	85.12 \pm 0.73	86.91 \pm 0.91	86.12 \pm 1.53
$AE \rightarrow A3: h_{src}, D_{src}:$	96.61 \pm 0.24	94.43 \pm 0.46	97.48 \pm 0.13
$AE \rightarrow A3: h_{src}, D_{tg}:$	98.17 \pm 0.20	96.49 \pm 0.48	90.40 \pm 1.16
$AE \rightarrow A3: h_{tg}, D_{tg}:$	70.91 \pm 0.87	60.50 \pm 0.54	50.00 \pm 1.06